Locally designed pulse shaping for selective preparation of enantiomers from their racemate

doi: 10.1063/1.1334867

Locally designed pulse shaping for selective preparation of enantiomers from their racemate

K. Hoki, Y. Ohtsuki, and Y. Fujimura
Department of Chemistry, Graduate School of Science, Tohoku University, Sendai 980-8578, Japan

(Received 14 August 2000; accepted 1 November 2000)

We present a method for the design of laser fields to control a selective preparation of enantiomers from their racemate. An expression for two components of the laser pulses [$E_X(t)$ and $E_Y(t)$] propagating along the Z axis is derived using a locally optimized control theory in the density operator formalism. This expression was applied to a selective preparation of (R-, L-) enantiomers from preoriented phosphinotioic acid (H_2POSH) at low temperatures. The target operator was set for the populations to be localized in one side of the double-well potential. First, a simple one-dimensional model was treated. Then, a two-dimensional model in which a free rotation around the preoriented torsional axis is included was briefly considered. In the one-dimensional model, almost complete preparation of the enantiomers was obtained. The optimal electric field consists of a sequence of two linearly polarized pulses with the same phases but with different magnitudes. This means that the resultant electric field is linearly polarized with the polarization for obtaining the R-form nearly parallel to its S–H bond. The optimal electric field transfers the L-form into the R-form while suppressing the reverse process. In the two-dimensional model, the enantiomer selective preparation is controlled by a sequence of circularly polarized pulses. © *2001 American Institute of Physics.* [DOI: 10.1063/1.1334867]

I. INTRODUCTION

Much interest has recently been shown in the selective preparation of enantiomers from their racemates in the fields of both chemical physics and in synthetic chemistry.[1] Various methods such as optical resolution or asymmetric synthesis have been developed for practical purposes.[2–5] Recently, new scenarios of selective preparation of enantiomers, which are based on quantum control or coherent control, have been proposed.[6–9] The first proposal of coherent control of enantiomer selective preparation was by Shapiro and Brumer.[6] In their scenario, enantiomer selection is performed by applying linearly polarized lasers to a prochiral molecule. A wave packet theory has been developed by Cina and Harris.[7] They have shown the possibility of preparation and phase control of superposition states of L- and R-enantiomers produced in an electronically excited state from a double-well potential in the ground state. A theory for controlling molecular chirality in chemical reactions by using circularly polarized fields has been presented by Shao and Hänggi.[8] Recently, Shapiro *et al.* proposed a new scenario for enantiomer control in a racemic mixture.[9] In their scenario a superposition of rovibronic states in a common excited electronic state of two enantiomers is manipulated to a desired enantiomer by a control laser.

In a previous study,[10] by applying a locally optimized control method, we achieved quantum control of an enantiomer selective preparation of preoriented phosphinotioic acid H_2POSH at a low temperature limit. In that study, we adopted a one-dimensional model. In this simple one-dimensional model, the torsion of SH around the PS bond is the reaction coordinate. Laser pulses were designed to convert the lowest, symmetric coherent achiral state of H_2POSH into a nonsymmetric localized state which represents a single enantiomer. H_2POSH is a molecule with axial chirality. This type of molecule has a memory of chirality that is called a dynamic chirality.[4] The duration of the memory of chirality of H_2POSH is 630 ps, which is equal to the tunneling time between two localized states, L- and R-forms in the ground torsional states.[10] Such a dynamic chirality of H_2POSH is controlled by two linearly polarized pulses [$E_X(t)$ and $E_Y(t)$]. The resultant pulses are elliptically or linearly polarized depending on the pulse intensity used. For example, in medium intensity cases, elliptically polarized electric fields are obtained as the optimal ones, which interact with H_2POSH adiabatically, and the symmetry of dipole moment functions and their magnitudes are reflected in the controlling electric fields. In a recent paper,[11] we presented a scenario for enantiomer control of H_2POSH from its racemic mixture using a sequence of pulses with analytical shapes.

In this article, we present a method for quantum control of enantiomer selective preparation of enantiomers from their racemate, starting from the equal mixture of L- and R-enantiomers at low temperature. For this purpose, we extend our locally designed pulse-shaping theory to the case of a mixed state by using the density operator formalism. We have developed locally designed pulse shaping theory that can be applicable not only to weak field cases but also to strong field cases.[12–15] Theoretical treatments of quantum control in density matrix formalism have been proposed by several groups.[16–21]

Before carrying out pulse shaping of enantiomer selective preparation from its racemate, we note two fundamental issues. The first one is associated with the choice of the target for population control in the mixed state. Accordingly,

we cannot localize a racemic mixture of molecules in the lowest state, i.e., complete enantiomer selection in the ground state can not be realized except for the case of an initial pure state. This restriction is based on the fact that the maximum value of the population transferred can not exceed the maximum value of the initial population distribution in a control system without any dissipative process, as shown by Gross *et al.*[22] This restriction to the population transfer can be understood from the unitary property of the density operator $\hat{\rho}(t)=U(t,t_0)\hat{\rho}(t_0)U^{\dagger}(t,t_0)$ where $\hat{\rho}(t_0)$ is the initial density operator that is diagonalized in the random phase approximation, and $U(t,t_0)$ is the time evolution operator. More specifically,

$$U(t,t_0)=T\exp\left[-\frac{i}{\hbar}\int_{t_0}^{t}dt' V_I(t')\right],$$

where T denotes a time-ordering operator and $V_I(t')$ is the interaction between molecules and controlling laser fields in the interaction representation. The eigenvalues of $\hat{\rho}(t)$ are thus invariant with respect to unitary transformation. The population of a state $|\xi\rangle$ in the target state at time t, $\langle\xi|\hat{\rho}(t)|\xi\rangle$, satisfies the condition that the minimum eigenvalue of $\hat{\rho}(t_0)\leqslant\langle\xi|\hat{\rho}(t)|\xi\rangle\leqslant$the maximum eigenvalue of $\hat{\rho}(t_0)$. That is, the maximum population in a target state at time t_f is equal to the maximum eigenvalue of the initial density operator $\hat{\rho}(t_0)$. According to this fundamental issue, we have to choose an alternative target operator for a selective preparation of enantiomers from their racemate, which involves not only ground but also excited states of the target enantiomer.

The second issue is associated with the ensemble of racemates from which enantiomers are selectively prepared by lasers. We note that enantiomers in a spherically symmetric (isotropic) ensemble, such as in a gas phase or in homogeneous solvents, can not be controlled by using lasers within the permanent dipole interaction, as adopted in most quantum control scenarios.[23] This can be proven by a symmetry consideration given next.

Consider an achiral (symmetric) ensemble whose density operator at the initial time $t=t_0$ is denoted by $\hat{\rho}(t_0)$. Here achiral means that $\hat{\rho}(t_0)$ is invariant with respect to operation of space inversion operator $\hat{P}$,[24] i.e., $\hat{P}\hat{\rho}(t_0)\hat{P}=\hat{\rho}(t_0)$. Now, let us assume that a density operator $\hat{\rho}_R$ of a system with R-form is produced by the permanent dipole interaction at $t=t_f$. The density operator, $\hat{\rho}_R$, is expressed in terms of the time evolution operator $U(t_f,t_0;\mathbf{E}(t))$ as $\hat{\rho}_R=U(t_f,t_0;\mathbf{E}(t))\hat{\rho}(t_0)U^{\dagger}(t_f,t_0;\mathbf{E}(t))$. Here the laser field $\mathbf{E}(t)$ is explicitly shown in $U(t_f,t_0;\mathbf{E}(t))$ to emphasize the initial phase dependence of the laser. Operation of $\hat{P}$ to $\hat{\rho}_R$ creates $\hat{\rho}_L=\hat{P}\hat{\rho}_R\hat{P}$, which is also expressed as $U(t_f,t_0;-\mathbf{E}(t))\hat{\rho}(t_0)U^{\dagger}(t_f,t_0;-\mathbf{E}(t))$. This result implies that the initial phase of the laser field should select a chiral system from an achiral ensemble. However, there are only few exceptional case studies demonstrating an initial phase dependence of femtosecond laser fields used in quantum control.[25] This means that, in most cases, the assumption adopted previously is invalid. In practice, it is extremely difficult, if not even impossible, to create a chiral system from an achiral ensemble through their dipole interaction.

This second issue thus implies that for application of quantum control techniques within the dipole approximation, it is necessary to introduce asymmetry into its ensemble of molecules, for example, by using preoriented racemates. Such an orientation can be realized by applying nonresonant intense laser pulses to symmetric system.[26–30] Under such a condition, linearly polarized pulses or elliptically (circularly) polarized pulses play the role of chiral reactants and transfer their chirality to molecules in racemic mixtures.

In the next section, we describe a control method for designing electric fields in the density operator formalism. In particular, we pay attention to how to obtain an expression for two optimal laser pulses, $E_X(t)$ and $E_Y(t)$, which are not independent of each other under the condition of their minimum energies supplied and whose optimal solution is given by a trajectory in the two-dimensional functional space. In Sec. III, we describe an application of the locally optimized method presented in Sec. II to H_2POSH under a preoriented condition at low temperature. First, we use the simple one-dimensional model that already has been used, and we then consider pulse shaping of H_2POSH in a two-dimensional model by taking into account the degree of freedom of molecular rotation. The mechanisms of the enantiomer selective preparation from its racemic mixture are discussed.

II. LOCAL CONTROL OF ENANTIOMER SELECTIVE PREPARATION IN THE DENSITY OPERATOR FORMALISM

Consider a selective preparation of enantiomers by using two linearly polarized pulses propagating along the Z axis in the space-fixed coordinates, whose electric fields are written as $E_X(t)$ for the X component and $E_Y(t)$ for the Y component. We outline the local control method for obtaining locally optimized pulses at finite temperatures. The density operator of the system $\hat{\rho}(t)$ satisfies the following equation:

$$i\hbar\frac{\partial\hat{\rho}(t)}{\partial t}=[\hat{H}(t),\hat{\rho}(t)]. \tag{1}$$

Here $\hat{H}(t)$, the total Hamiltonian, is given by

$$\hat{H}(t)=\hat{H}_M-\hat{\mu}_X E_X(t)-\hat{\mu}_Y E_Y(t). \tag{2}$$

The first term on the right-hand side, $\hat{H}_M$, is the molecular Hamiltonian and the other terms are interactions between molecules and control fields in the dipole approximation. μ_X and μ_Y are the X and Y components of the dipole moment, respectively. The objective functional $J\{E_X(t),E_Y(t)\}$ is defined as

$$J\{E_X(t),E_Y(t)\}=\mathrm{Tr}\{\hat{\rho}(t_f)\hat{W}\}-\frac{1}{\hbar A}\int_{t_0}^{t_f}dt[E_X(t)^2+E_Y(t)^2]. \tag{3}$$

Here the first term on the right-hand side is the average of the target operator $\hat{W}$ over the distribution at a fixed time t

$=t_f$. The second term represents the penalty of the energy of the control laser pulses. A is a parameter specifying the magnitude of the electric field energy.

The objective function is rewritten in the integral form as

$$J\{E_X(t),E_Y(t)\}=\int_{t_0}^{t_f}dtg(t)+\mathrm{Tr}\{\hat{\rho}(t_0)\hat{W}\}. \tag{4}$$

Here $g(t)$ is expressed as

$$g(t)=\frac{d}{dt}\mathrm{Tr}\{\hat{\rho}(t)\hat{W}\}-\frac{1}{\hbar A}[E_X(t)^2+E_Y(t)^2]. \tag{5}$$

The condition for the local optimization is given by $g(t)=0$.[14] Local control optimization means that the rate of the expectation value of the target operator is positive and is proportional to the laser intensity at each time. In other words, there is no memory effect, and the wavepacket motion is determined at each time when the electric fields interact with the system. That is, Eq. (5) is expressed as

$$\frac{d}{dt}\mathrm{Tr}\{\hat{\rho}(t)\hat{W}\}=\frac{1}{\hbar A}[E_X(t)^2+E_Y(t)^2]\geqslant 0. \tag{6}$$

In global optimization, on the other hand, memory effects are taken into account by evaluating the forward and backward wavepacket propagation.

Equation (5) is rewritten as

$$\begin{aligned}g(t)=&\frac{i}{\hbar}\mathrm{Tr}\{\hat{\rho}(t)[\hat{H}_M,\hat{W}]\}-\frac{1}{\hbar A}[E_X(t)^2\\&+2A\,\mathrm{Im}\,\mathrm{Tr}\{\hat{\rho}(t)\hat{W}\hat{\mu}_X\}E_X(t)+E_Y(t)^2\\&+2A\mathrm{Im}\,\mathrm{Tr}\{\hat{\rho}(t)\hat{W}\hat{\mu}_Y\}E_Y(t)]=0\end{aligned} \tag{7}$$

where $[\,,\,]$ is a commutator. This leads to

$$\mathrm{Tr}\{\hat{\rho}(t)[\hat{H}_M,\hat{W}]\}=0, \tag{8}$$

and

$$\begin{aligned}&[E_X(t)+A\,\mathrm{Im}\,\mathrm{Tr}\{\hat{\rho}(t)\hat{W}\hat{\mu}_X\}]^2\\&\quad+[E_Y(t)+A\,\mathrm{Im}\,\mathrm{Tr}\{\hat{\rho}(t)\hat{W}\hat{\mu}_Y\}]^2\\&\quad=(A\,\mathrm{Im}\,\mathrm{Tr}\{\hat{\rho}(t)\hat{W}\hat{\mu}_X\})^2+(A\,\mathrm{Im}\,\mathrm{Tr}\{\hat{\rho}(t)\hat{W}\hat{\mu}_Y\})^2.\end{aligned} \tag{9}$$

It should be noted that $E_X(t)$ and $E_Y(t)$ are not independent of each other. From Eq. (9), solutions of $E_X(t)$ and $E_Y(t)$ for local control are given by a circle in a two-dimensional space. To determine the optimal solution for each electric field uniquely, we impose the additional condition under which the electric fields give the maximum rate of the expectation value, $(d/dt)\mathrm{Tr}\{\hat{\rho}(t)\hat{W}\}_{\max}$.

The conditions for our local optimal electric fields have an illustrating geometric interpretation. Figure 1 shows two circles that come into contact at one point on the two-dimensional electric field surface. One is a circle with a radius of $\{(A\,\mathrm{Im}\,\mathrm{Tr}\{\hat{\rho}(t)\hat{W}\hat{\mu}_X\})^2+(A\,\mathrm{Im}\,\mathrm{Tr}\{\hat{\rho}(t)\hat{W}\hat{\mu}_Y\})^2\}^{1/2}$ around its center $(-A\,\mathrm{Im}\,\mathrm{Tr}\{\hat{\rho}(t)\hat{W}\hat{\mu}_X\}$, $-A\,\mathrm{Im}\,Tr\{\hat{\rho}(t)\hat{W}\hat{\mu}_Y\})$, and the other is a circle around the origin (0, 0) with a radius $\{\{\hbar A(d/dt)\mathrm{Tr}\{\hat{\rho}(t)\hat{W}\}_{\max}\}^{1/2}$. In

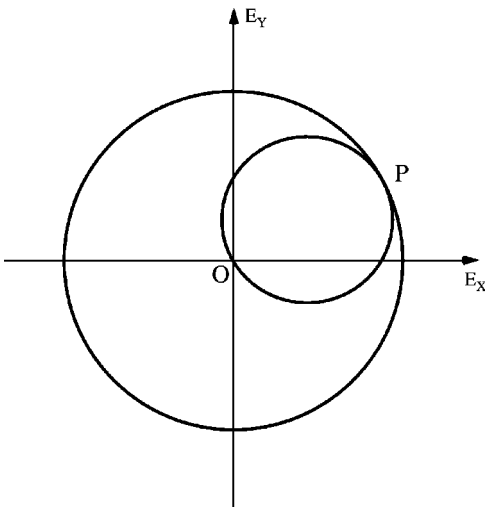

FIG. 1. Two-dimensional electric field $[E_X(t)$and $E_Y(t)]$ surface for giving the expression for locally optimized electric fields. The optimized fields are located at the point P at which the two circles come into contact. The radius of the outer circle corresponds to the maximum rate of the expectation value of the target operator, and the inner circle denotes solutions of the locally optimized pulses.

Fig. 1, the inner circle denotes solutions of the locally optimized pulses, which is given by Eq. (9). One trivial solution is given by $E_X(t)=0$ and $E_Y(t)=0$, which is involved at the origin of the figure. The outer circle denotes the contour of the intensity of the electric fields whose radius gives the maximum rate of the expectation value of the target operator $\hat{W}$, $(d/dt)\mathrm{Tr}\{\hat{\rho}(t)\hat{W}\}_{\max}$, at the point P.

The optimal control pulses $E_X(t)$ and $E_Y(t)$ are given by the point P at which the two circles come into contact. That is, the locally optimized control fields are expressed as

$$E_X(t)=-2A\,\mathrm{Im}\,\mathrm{Tr}\{\hat{\rho}(t)\hat{W}\hat{\mu}_X\} \tag{10a}$$

and

$$E_Y(t)=-2A\,\mathrm{Im}\,\mathrm{Tr}\{\hat{\rho}(t)\hat{W}\hat{\mu}_Y\}. \tag{10b}$$

Because of the restriction in locally optimized control, given by Eq. (8), i.e., the target operator should commute with the free-field molecular Hamiltonian, a backward time-propagation method is adopted.[14] The target operator for the backward propagation is given as the diagonal density operator in the mixed state, which is the density operator at the initial time t_0. The initial state for the backward propagation is taken as the state that corresponds to the final target state for the forward propagation.

III. APPLICATION TO H_2POSH

A. One-dimensional model

Consider an enantiomer selective preparation of H_2POSH in a one-dimensional model as shown in Fig. 2.

The initial distribution $\hat{\rho}(t_0)$ is assumed to be a Boltzmann distribution,

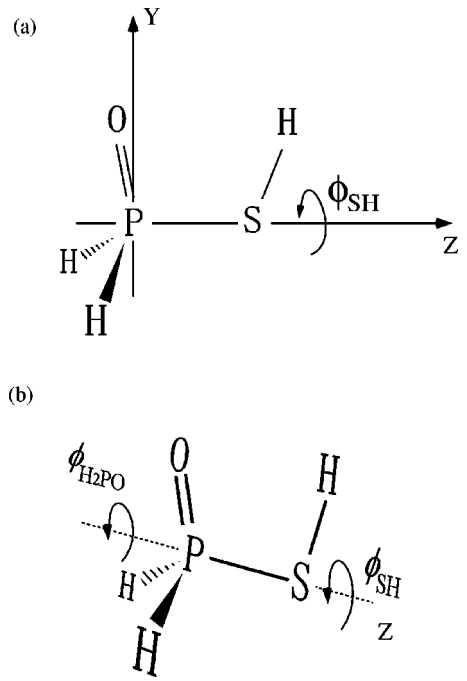

FIG. 2. Geometry of H_2POSH in (a) a one-dimensional model and (b) a two-dimensional model.

$$\hat{\rho}(t_0)=\frac{\exp(-\hat{H}_M/kT)}{\mathrm{Tr}[\exp(-\hat{H}_M/kT)]}, \tag{11}$$

where k denotes the Boltzmann constant and T is the temperature.

Taking into account the torsional energy level structure of H_2POSH, in which the energy gap between the lowest state $|0+\rangle$ and the first excited state $|0-\rangle$ is about 0.05 cm^{-1} and that between $|0+\rangle$ and the second excited state $|1+\rangle$ and the third excited state $|1-\rangle$ is about 200 cm^{-1},[10] we assumed that in a low temperature limit, the initial density operator is given by

$$\hat{\rho}(t_0)=|0+\rangle\tfrac{1}{2}\langle 0+|+|0-\rangle\tfrac{1}{2}\langle 0-|, \tag{12}$$

that is, only two states, $|0+\rangle$ and $|0-\rangle$, are populated, and they are equally distributed. The localized states, $|\nu R\rangle$ ($\nu=0$ and 1) which are localized in a well in the right-hand side and $|\nu L\rangle$ which are localized into the left well are expressed as

$$|\nu R\rangle=\frac{1}{\sqrt{2}}(|\nu+\rangle-|\nu-\rangle) \tag{13a}$$

and

$$|\nu L\rangle=\frac{1}{\sqrt{2}}(|\nu+\rangle+|\nu-\rangle), \tag{13b}$$

respectively.

The initial density operator, Eq. (12), can be rewritten in terms of the localized basis, Eq. (13), as

$$\hat{\rho}(t_0)=|0R\rangle\tfrac{1}{2}\langle 0R|+|0L\rangle\tfrac{1}{2}\langle 0L|. \tag{14}$$

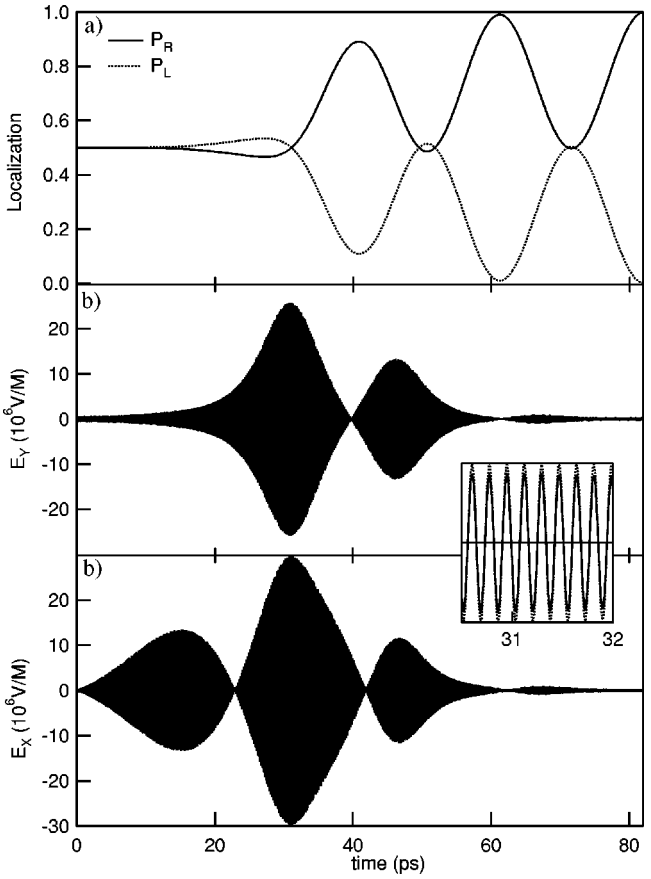

FIG. 3. (a) Population changes in enantiomers localized on the R-well (solid curve) and L-well (dotted curve). (b) Locally designed pulse shapes for controlling the enantiomer selective preparation in a mixed state. The upper and lower figures show the pulse shapes of $E_X(t)$ and $E_Y(t)$, respectively. The inserted figure shows the expanded view of $E_X(t)$ (solid line) and $E_Y(t)$ (dotted line). These electric fields are characterized by their same phase.

Equation (14) expresses a racemic mixture in the initial state since the L-form and R-form are equally populated.

We now specify the target operator $\hat{W}$ for enantiomer selection. As already described in the Introduction, the largest population transferred by optimal pulses cannot exceed the maximum eigenvalue of $\hat{\rho}(t_0)$. In the present enantiomer selection, there are two nonzero eigenvalues of $\frac{1}{2}$, which is the maximum eigenvalue of $\hat{\rho}(t_0)$. Let the target population be localized in one of the wells, e.g., to produce the R-form of H_2POSH. Since the transformation between the eigenstate representation and the localized state representation is unitary, the eigenvalues are invariant under the transformation. The choice of the target operator is not unique. In this study, we chose

$$\hat{W}=|0R\rangle\tfrac{1}{2}\langle 0R|+|1R\rangle\tfrac{1}{2}\langle 1R| \tag{15}$$

as the target operator since his gives the lowest energy of the mixed system in the final product.

Figure 3(a) shows the time-development of the localization of enantiomers to the R-form, which is calculated by the locally optimized control method. The solid and dotted curves in Fig. 3(a) are population changes in H_2POSH with the R- and L-forms, respectively. We can see that there is

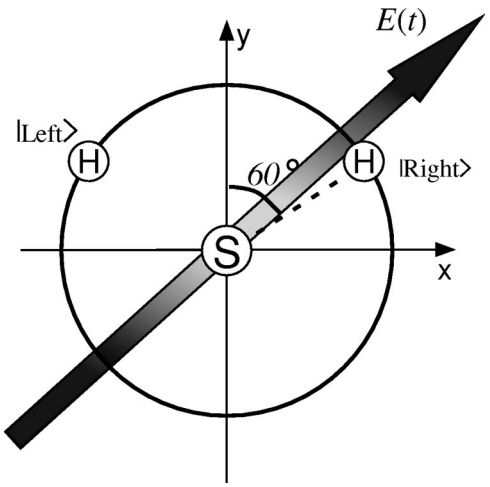

FIG. 4. The optimal electric field polarization synthesized by the two electric fields shown in Fig. 3. Two enantiomer configurations of the R- and L-forms are shown as well.

almost complete localization within 60 ps. The oscillation in Fig. 3(a) whose period is of 21 ps originates from the frequency difference of 1.6 cm^{-1} between $|1+\rangle$ and $|1-\rangle$ states.[10]

Figure 3(b) shows the optimal pulses for the localization of the enantiomers in Fig. 3(a). The upper (solid) and lower (dotted) curves represent the pulse shapes of $E_X(t)$ and $E_Y(t)$, respectively. The expanded view of the two electric fields between 30.5 and 32.0 ps is also shown in the inserted figure. The two electric fields consist of the central frequency of $\sim$200 cm^{-1}, which correspond to transition frequencies between $|0\pm\rangle$ and $|1\pm\rangle$. Figure 3(b) also shows that the two electric fields have the same phase with different magnitudes, which means the synthesized electric field is a linearly polarized one oriented about 60° with respect to the *YZ* plane as shown in Fig. 4. This orientation of the electric fields is close to that of the R-form in the equilibrium configuration.

Figure 4 shows the polarization direction of the optimal field together with the two configurations, the R- and L-forms. The polarization of the synthesized electric field is parallel to the S–H bond of the R-form. This means that the resultant field has the ability to transfer the L-form into the R-form while suppressing its reverse process. This is the mechanism of the enantiomer selective preparation of H_2POSH in the mixed state.

In a previous paper,[11] we proposed a control scenario of enantiomer preparation from its racemates by a sequence of analytical pulses. It is interesting to compare the results of this study with those obtained by the analytical method. The electric fields designed by the optimal control method are approximated by a sequence of Gaussian pulses similar to those used in an analytical treatment, but the electric fields in the former are smaller than those in the latter by one to two orders of magnitudes. This difference in the magnitudes of the fields originates mainly from the mechanisms adopted. The present study yields dominant transitions between four-levels, in comparison with five-levels in the analytical treatment. The difference also originates partly from the setting of the final time t_f: t_f = 60 ps in the present study and t_f = $\sim$40 ps for the analytical treatment.

So far we have demonstrated the selective preparation of the R-form from its racemates. To selectively prepare L-enantiomers from their racemates, we need two electric fields with the relative phase of $-\pi$. This means the resultant field is a linearly polarized field whose polarization is oriented by $-60°$.

B. Two-dimensional model

We now briefly consider quantum control of prealigned H_2POSH by taking into account the degree of molecular rotations. For simplicity, we restrict ourselves to the molecular rotation around the principal *Z* axis as shown in Fig. 2. The model Hamiltonian including the molecular rotation, $\hat{H}(t)$, is expressed as

$$\hat{H}(t) = -\frac{\hbar^2}{2I_{\mathrm{HS}}}\frac{\partial^2}{\partial\phi_{\mathrm{HS}}^2} - \frac{\hbar^2}{2I_{\mathrm{H_2PO}}}\frac{\partial^2}{\partial\phi_{\mathrm{H_2PO}}^2} + V(\phi_{\mathrm{HS}}-\phi_{\mathrm{H_2PO}}) - \mu_X(\phi_{\mathrm{HS}},\phi_{\mathrm{H_2PO}})E_X(t) - \mu_Y(\phi_{\mathrm{HS}},\phi_{\mathrm{H_2PO}})E_Y(t). \tag{16}$$

Here ϕ_{HS} and $\phi_{\mathrm{H_2PO}}$ are the angles of the HS and H_2PO groups around the PS bond measured from the *X* axis in space-fixed Cartesian coordinates, respectively, as shown in Fig. 2. I_{HS} and $I_{\mathrm{H_2PO}}$ are the moments of inertia of the HS and H_2POSH groups, respectively. The OP bond of H_2POSH is taken to be in the y/z plane of the molecular-fixed Cartesian coordinates. The reaction coordinate of the enantiomer selective preparation is given as $\phi=\phi_{\mathrm{HS}}-\phi_{\mathrm{H_2PO}}$. μ_X and μ_Y are, respectively, the *X* and *Y* components of the dipole moment functions defined in the space-fixed coordinates, and they are related to those defined in molecular-fixed coordinates, x,y and depending on the reaction coordinate through

$$\begin{pmatrix} \mu_X(\phi_{\mathrm{HS}},\phi_{\mathrm{H_2PO}}) \\ \mu_Y(\phi_{\mathrm{HS}},\phi_{\mathrm{H_2PO}}) \end{pmatrix} = \begin{pmatrix} \cos(\phi_{\mathrm{H_2PO}}) & -\sin(\phi_{\mathrm{H_2PO}}) \\ \sin(\phi_{\mathrm{H_2PO}}) & \cos(\phi_{\mathrm{H_2PO}}) \end{pmatrix} \times \begin{pmatrix} \mu_x(\phi_{\mathrm{HS}}-\phi_{\mathrm{H_2PO}}) \\ \mu_y(\phi_{\mathrm{HS}}-\phi_{\mathrm{H_2PO}}) \end{pmatrix}. \tag{17}$$

The angular momentum operator of the rotation, $\hat{J}$, is defined as

$$\hat{J}_Z = -i\hbar\left(\frac{\partial}{\partial\phi_{\mathrm{HS}}} + \frac{\partial}{\partial\phi_{\mathrm{H_2PO}}}\right), \tag{18}$$

since

$$\exp[-i\alpha\hat{J}_Z]\psi(\phi_{\mathrm{HS}},\phi_{\mathrm{H_2PO}}) = \psi(\phi_{\mathrm{HS}}+\alpha,\phi_{\mathrm{H_2PO}}+\alpha), \tag{19}$$

where ψ is the wave function of H_2POSH in the two-dimensional model. The molecular Hamiltonian including the molecular rotation, $\hat{H}_M$, and $\hat{J}_Z$ satisfies the commutation relation

$$[\hat{H}_M, \hat{J}_Z] = 0. \tag{20}$$

The quantum number of $\hat{J}_Z$ is denoted by M (= 0, ± 1, ± 2, ± 3,...). The basis set in the two-dimensional model is denoted by $|\nu\pm, M\rangle$. The energies of the eigenstates $|\nu\pm, M\rangle$ are approximated by

$$E_{\nu\pm,M} \approx E_{\nu\pm} + \frac{\hbar^2}{2I} M^2, \tag{21}$$

where I is the moment of inertia of H_2POSH, and the values of $\hbar^2/2I$ in units of cm^{-1} is 0.58.

Consider the simplest case in which $M=0$ under a low temperature condition. We set the initial density operator as

$$\hat{\rho}(t_0) = |0+,0\rangle \tfrac{1}{2} \langle 0+,0| + |0-,0\rangle \tfrac{1}{2} \langle 0-,0|, \tag{22}$$

since the energy differences both between two states $|0-,1\rangle$ and $|0-,0\rangle$ and between $|0+,1\rangle$ and $|0+,0\rangle$ are larger than the energy difference between $|0+,0\rangle$ and $|0-,0\rangle$. We set the target operator as

$$\hat{W} = |0R,0\rangle \tfrac{1}{2} \langle 0R,0| + |1R,1\rangle \tfrac{1}{2} \langle R,1|. \tag{23}$$

Here localized states, the R(L)-forms of the enantiomer $|\nu R, M\rangle (|\nu L, M\rangle)$ are expressed in a similar way to that in Eq. (13) as

$$|\nu R, M\rangle = \frac{1}{\sqrt{2}} (|\nu+, M\rangle - |\nu-, M\rangle), \tag{24a}$$

$$|\nu L, M\rangle = \frac{1}{\sqrt{2}} (|\nu+, M\rangle + |\nu-, M\rangle). \tag{24b}$$

Figure 5(a) shows the time-development of the localization of enantiomers to the R-form starting from its racemate. Here $|\nu\pm, M\rangle$ with $\nu = 0,1,2,3$ and $|M| = 0,1,2,3$ was used as the basis set. Solid and broken curves denote the population of the R-form and L-form, respectively. We can see from Fig. 5 that ~60% of the R-form is produced within ~100 ps. Thus, inclusion of molecular rotation reduces the ability of enantiomer selection compared with that of the one-dimensional case. If we use pulses with a long duration, we can obtain as efficient an enantiomer selection as that in the case of the previous one-dimensional model. However, we are interested in enantiomer control within shorter time regime than the tunneling time of 630 ps in the present model system.

Figure 5(b) shows the optimal fields controlling the enantiomer selection. The control pulses consist of central frequency of ~200 cm^{-1}, which corresponds to the transition frequencies between $|0\pm,0\rangle$ to $|1\pm,1\rangle$, and consists of a sequence of circularly polarized pulses, i.e., the phase difference between two pulses, $E_X(t)$ and $E_Y(t)$, is $\pi/2$, and their amplitudes are equal to each other, as shown in the inserted figure of Fig. 5. This is because the selection rule for one-photon transitions between two rotational states is given by $\Delta M = \pm 1$ in the two-dimensional model, and such transitions are induced by circularly polarized pulses. By applying such a circularly polarized pulse to racemates a transition ($M = 1 \leftarrow M = 0$ for a right circularly polarized pulse, or $M = -1 \leftarrow M = 0$ for a left circularly polarized one) is induced,

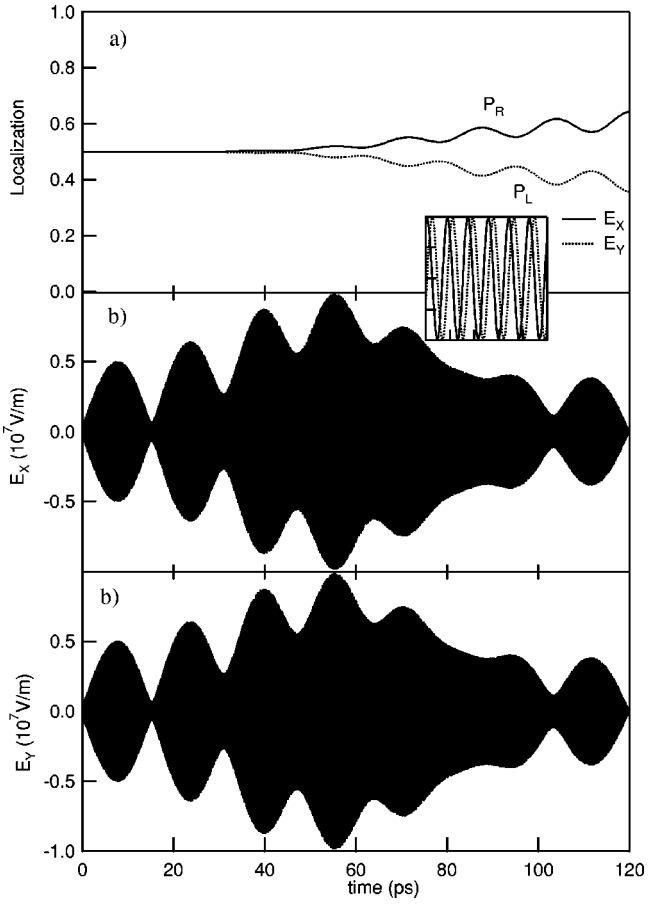

FIG. 5. (a) Time development of localization of enantiomers to the R-form in the two-dimensional model. Solid and broken curves denote the populations of the R-form and L-form, respectively. (b) Locally designed pulses in the 2-dimensional model. The upper and lower figures show the pulse shapes of $E_X(t)$ and $E_Y(t)$, respectively. The inserted figure shows the expanded view of $E_X(t)$ (solid line) and $E_Y(t)$ (dotted line). These electric fields are $\pi/2$ phase shifted, i.e., the resultant field is a circularly polarized one.

and the coherent super position of the eigenstates, i.e., R(L)-enantiomer, is created on the same well as that in the initial state.

IV. CONCLUSION

In order to carry out quantum control of the selective preparation of enantiomers from racemates, we have derived an expression for the optimal electric fields of two linearly polarized pulses in the density operator formalism. The treatment is an extension of a locally optimized pulse shaping method. We applied the method to the enantiomer selective preparation of pre-oriented or pre-aligned H_2POSH from its racemates in both simple, one- and two-dimensional models. The controlling field in a nonrotating one-dimensional case consists of a sequence of two linearly polarized pulses with their same phase. The polarization of the optimized electric field is parallel to the S–H bond of the R-enantiomer. The resultant field has the ability to transfer the L-enantiomers into R-enantiomers while suppressing its reverse process. In the case of a two-dimensional model, the rotational degree of freedom of enantiomers for rotation around the torsional axis

is taken into account. The optimal field calculated in the case in which $M=0$ consists of a sequence of circularly polarized pulses.

ACKNOWLEDGMENTS

We would like to thank Professor J. Manz for stimulating discussion, fruitful comments and pertinent suggestion. We gratefully acknowledge Professor P. Hänggi and Professor R. A. Harris for their critical comments on our preliminary work related to this article. This work was partly supported by a German–Japanese International Joint research project, by Grants-in-Aid for Scientific Research (No. 10640480) and by Grant-in-Aid for Scientific Research on Priority Area (No. 11166205).

[1] M. Avalos, R. Babiano, P. Cintas, J. Jimenez, J. C. Palacios, and L. D. Barron, Chem. Rev. **98**, 2391 (1998).
[2] Y. Inoue, Chem. Rev. **92**, 741 (1992).
[3] R. Noyori, *Asymmetric Catalysis in Organic Synthesis* (Wiley, New York, 1994).
[4] A. E. Rowan and R. J. M. Nolte, Angew. Chem. Int. Ed. Engl. **37**, 63 (1998).
[5] K. Fuji and T. Kawabata, Chem. Eur. J. **4**, 373 (1998).
[6] M. Shapiro and P. Brumer, J. Chem. Phys. **95**, 8658 (1991).
[7] J. A. Cina and R. A. Harris, J. Chem. Phys. **100**, 2531 (1994); Science **267**, 832 (1995).
[8] J. Shao and P. Hänggi, J. Chem. Phys. **107**, 9935 (1997); Phys. Rev. A **56**, R4397 (1997).
[9] M. Shapiro, E. Frishman, and P. Brumer, Phys. Rev. Lett. **84**, 1669 (2000).
[10] Y. Fujimura, L. González, K. Hoki, J. Manz, and Y. Ohtsuki, Chem. Phys. Lett. **306**, 1 (1999); **310**, 578 (1999).
[11] Y. Fujimura, L. González, K. Hoki, D. Kröner, J. Manz, and Y. Ohtsuki, Angew. Chem. (in press).
[12] M. Sugawara and Y. Fujimura, J. Chem. Phys. **100**, 5646 (1994).
[13] Y. Watanabe, H. Umeda, Y. Ohtsuki, H. Kono, and Y. Fujimura, Chem. Phys. **217**, 317 (1997).
[14] Y. Ohtsuki, H. Kono, and Y. Fujimura, J. Chem. Phys. **109**, 9318 (1998).
[15] H. Umeda and Y. Fujimura, J. Chem. Phys. **113**, 3510 (2000).
[16] Y. Yan, R. E. Gillian, R. M. Whitnell, K. R. Wilson, and S. Mukamel, J. Phys. Chem. **97**, 2320 (1993).
[17] M. Sugawara and Y. Fujimura, J. Chem. Phys. **101**, 6586 (1994).
[18] O. Kühn, D. Malzahn, and V. May, Int. J. Quant. Chem. **57**, 343 (1996).
[19] M. V. Korolkov, J. Manz, and G. K. Paramonov, J. Phys. Chem. **101**, 13927 (1995).
[20] Y. Ohtsuki, W. Zhu, and H. Rabitz, J. Chem. Phys. **110**, 9825 (1999).
[21] J. M. Yuan, W-K. Liu, M. Hayashi, and S. H. Lin, J. Chem. Phys. **110**, 3828 (1999).
[22] P. Gross, D. Neuhauser, and H. Rabitz, J. Chem. Phys. **94**, 1158 (1991).
[23] C. S. Maierle and R. A. Harris, J. Chem. Phys. **109**, 3713 (1998).
[24] M. Quack, *Femtosecond Chemistry, Vol. 2*, edited by J. Manz and L. Wöste (VCH, Weinheim, 1995), p. 781.
[25] M. V. Korolkov, J. Manz, and G. K. Paramnov, Chem. Phys. **217**, 341 (1997).
[26] B. Friedrich and D. Herschbach, Phys. Rev. Lett. **74**, 4623 (1995).
[27] H. Sakai, C. P. Sufvan, J. J. Larsen, K. M. Hillingsoe, K. Hald, and H. Stapelfeldt, J. Chem. Phys. **110**, 10235 (1999).
[28] C. M. Dion, A. D. Bandrauk, O. Akabek, A. Keller, H. Umeda, and Y. Fujimura, Chem. Phys. Lett. **302**, 215 (1999).
[29] A. Sugita, M. Mashino, M. Kawasaki, Y. Matsumoi, R. J. Gordon, and R. Bersohn, J. Chem. Phys. **112**, 2164 (2000).
[30] T. Seideman, Phys. Rev. Lett. **83**, 4971 (1999).